The ISME Journal (2008) 2, 663–676
© 2008 International Society for Microbial Ecology All rights reserved 1751-7362/08 $30.00
www.nature.com/ismej

ORIGINAL ARTICLE

Nitrogen fixation in an anticyclonic eddy in the oligotrophic North Pacific Ocean

Allison A Fong[1], David M Karl[1], Roger Lukas[1], Ricardo M Letelier[2,3], Jonathan P Zehr[4] and Matthew J Church[1]

[1]*Department of Oceanography, University of Hawaii, Honolulu, HI, USA;* [2]*College of Oceanic and Atmospheric Sciences, Oregon State University, Corvallis, OR, USA;* [3]*Center for Advanced Studies in Ecology and Biodiversity, Department of Ecology, Pontifícia Universidad Católica de Chile, Casilla, Santiago, Chile and* [4]*Ocean Sciences Department, University of California Santa Cruz, Santa Cruz, CA, USA*

Mesoscale physical processes (for example eddies, frontal meanders and planetary waves) can play important roles in controlling ocean biogeochemistry. We examined spatial variations in upper ocean (0–100 m) nutrient inventories, N_2 fixing microorganism diversity and abundance, and rates of N_2 fixation in an anticyclonic eddy near Station ALOHA (22° 45′ N, 158° 00′ W) in the North Pacific Subtropical Gyre (NPSG). In July 2005, satellite-based sea surface altimetry and ocean color observation revealed an anticyclonic eddy with enhanced chlorophyll in the upper ocean in the vicinity of Station ALOHA. Within the eddy, near-surface ocean chlorophyll concentrations were ~5-fold greater than in the surrounding waters. Inventories of nitrate and phosphate in the eddy were similar to the concentrations historically observed at Station ALOHA, while silicic acid inventories were significantly depleted (one-way analysis of variance, $P<0.01$). Quantitative PCR determinations of *nifH* gene copies revealed relatively high abundances of several N_2 fixing cyanobacteria, including *Trichodesmium* spp., *Crocosphaera watsonii* and *Richelia intracellularis*. Reverse transcriptase PCR (RT-PCR) amplified nitrogenase (*nifH*) gene transcripts were cloned and sequenced to examine the diversity of active N_2 fixing microorganisms; these clone libraries were dominated by sequence-types 97%–99% identical to the filamentous cyanobacteria *Trichodesmium* spp. Near-surface ocean rates of N_2 fixation were 2–18 times greater (averaging 8.6 ± 5.6 nmol N per l per day) than previously reported measurements at Station ALOHA. These results suggest that mesoscale physical variability can play an important role in modifying the abundances of N_2 fixing microorganisms and associated rates of N_2 fixation in open ocean ecosystems.

The ISME Journal (2008) **2,** 663–676; doi:10.1038/ismej.2008.22; published online 28 February 2008
Subject Category: microbial ecology and functional diversity of natural habitats
Keywords: nitrogen fixation; eddy; mesoscale; North Pacific Ocean; *nifH*

Introduction

In open ocean ecosystems, mesoscale (100–200 km) physical processes such as eddies and planetary waves play important roles in controlling plankton productivity and altering plankton community structure. Oceanic eddies are transient, rotating parcels of seawater (~50–200 km in diameter) that form as a consequence of flow instabilities. Planetary waves (also termed Rossby waves) are westward propagating waves, oscillating with wavelengths of 100s to 1000s of kilometers, that are forced by variations in wind stress curl. Both eddies and waves can vertically displace the thermocline by 10s to 100s of meters, thereby influencing nutrient availability and plankton metabolism in the upper ocean (Falkowski *et al.*, 1991; Allen *et al.*, 1996; McGillicuddy *et al.*, 1998; Letelier *et al.*, 2000; Sweeney *et al.*, 2003; Sakamoto *et al.*, 2004). However, the spatial and temporal scales over which mesoscale processes alter plankton diversity and population abundances are not well understood, limited in part by undersampling of such features.

In large regions of the world's oceans, concentrations of bioessential nutrients in the well-lit upper ocean are vanishingly low (nanomolar concentrations). At Station ALOHA, the field site of the Hawaii Ocean Time-Series (HOT) program, near-surface concentrations of nitrate + nitrite (N + N) and soluble reactive phosphorus (SRP) range from 1 to 10 and 10 to 50 nmol l^{-1}, respectively (Karl *et al.*, 2001). Historically, the introduction of fixed nitrogen (N) to near-surface waters was thought to be largely restricted to vertical diffusion, advection and

Correspondence: MJ Church, Department of Oceanography, University of Hawaii, 1000 Pope Road, Honolulu, HI 96822, USA. E-mail: mjchurch@hawaii.edu
Received 26 November 2007; revised 1 February 2008; accepted 1 February 2008; published online 28 February 2008

mixing. However, various groups of marine bacteria are capable of reducing dinitrogen (N_2) to ammonia, providing a source of fixed N input to upper ocean ecosystems independent of vertical exchanges. Biological N_2 fixation is catalyzed by the nitrogenase enzyme, a complex consisting of two multisubunit proteins: dinitrogenase reductase, encoded by the *nifH* gene, and dinitrogenase, encoded by the *nifD* and *nifK* genes (Postgate, 1982).

Over the past several decades, numerous studies have focused on understanding the importance of N_2 fixation to ocean N budgets. Direct measurements and modeling determinations indicate N_2 fixation forms an important component of new N input throughout much of the tropical and subtropical oceans (Lipschultz and Owens, 1996; Michaels *et al.*, 1996; Gruber and Sarmiento, 1997; Karl *et al.*, 1997; Deutsch *et al.*, 2001; Capone *et al.*, 2005). Additionally, time series analyses of particulate N export at Station ALOHA in the North Pacific Subtropical Gyre (NPSG) imply N_2 fixation accounts for more than one-half of the total N export from the ecosystem (Karl *et al.*, 1997; Dore *et al.*, 2002). Much of our understanding of N_2 fixation derives from laboratory and field studies on *Trichodesmium*, a filamentous cyanobacterium ubiquitous throughout tropical and subtropical oceans. However, more recent use of molecular tools has provided insight into the diversity and spatial distributions of N_2 fixing microorganisms in the oceans (Zehr *et al.*, 1998, 2001; Church *et al.*, 2005b; Foster and Zehr, 2006).

Various lines of evidence suggest that episodic mesoscale events, such as those controlled by baroclinic eddies and short Rossby waves, may form an important component of the annual N fluxes within oligotrophic ocean gyres (McGillicuddy *et al.*, 1998, 1999; McNeil *et al.*, 1999; Letelier *et al.*, 2000; Uz *et al.*, 2001; Sakamoto *et al.*, 2004). To date, however, the influences of such mesoscale events on plankton ecology and biogeochemistry remain poorly understood, in part, due to their stochastic nature and a chronic undersampling of these features. The formation and evolution of mesoscale eddies and planetary waves can vertically perturb density surfaces for extended periods (weeks to months) relative to downwelling radiation, thereby potentially inducing ecosystem responses through alteration of nutrient and light fields. Biological utilization of nutrients introduced to the upper water column is often rapid (hours to days), while nutrient supply mechanisms function on the order of weeks to months (McGillicuddy and Robinson, 1997). This juxtaposition of time scales challenges our ability to correlate mesoscale biological responses with physical features.

In the current study, we examined spatial variability in N_2 fixing microorganism community structure and biogeochemistry within an anticyclonic eddy in the oligotrophic North Pacific Ocean. Our results indicate that anticyclonic eddies may play important roles in structuring diazotroph assemblages and controlling variability in rates of N_2 fixation in the open ocean.

Materials and methods

Satellite observations and shipboard sampling

To evaluate spatial variability in the biogeochemical structure of the eddy, a shipboard sampling transect was conducted that bisected the region of enhanced chlorophyll (Figure 1). Samples were collected along the transect at 11 stations located in close proximity to Station ALOHA; samples were collected over a 24 h period beginning July 26 2005 (Table 1). Prior to the cruise, a large ($\sim$35 000 km^2) coherent region of enhanced sea surface chlorophyll southeast of Station ALOHA was observed via the Moderate Resolution Imaging Spectroradiometer (MODIS) ocean color satellite. Surface chlorophyll data for the region surrounding Station ALOHA were derived from the MODIS ocean color sensor onboard Aqua. Eight-day composites of surface chlorophyll *a* images for the region were calculated using a running average on daily 4 km resolution

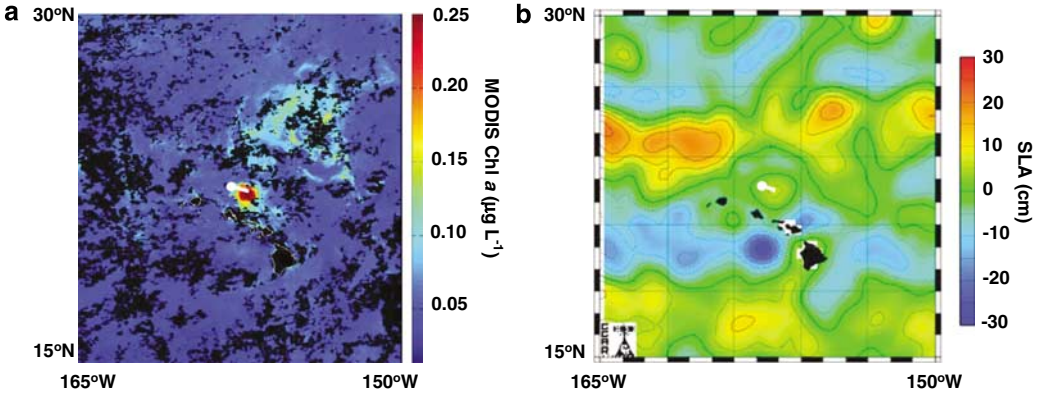


Figure 1 (**a**) Eight-day composite of satellite-derived near-surface ocean chlorophyll and (**b**) satellite-derived SLA in the vicinity of Station ALOHA (22° 45′ N, 158° W) for 22 July 2005. Sampling transect depicted by solid white line; Station ALOHA is shown by white circle. SLA, sea level anomaly.

Table 1 Depth-integrated (0–100 m) nutrient and pigment inventories and ratios at different stations sampled within the anticyclonic eddy; station numbers increase from eddy center to leading edge

	HOT 171	*Station 4*	*Station 5*	*Station 6*	*Station 7*	*Station 8*	*Station 9*	*Station 10*	*Station 11*	*HOT 172*
Location	22° 45′ N, 158° W	22° 22′ N, 157° 30′ W	22° 27′ N, 157° 39′ W	22° 33′ N, 157° 48′ W	22° 35′ N, 157° 53′ W	22° 38′ N, 157° 57′ W	22° 41′ N, 158° 03′ W	22° 45′ N, 158° 09′ W	22° 50′ N, 158° 18′ W	22° 45′ N, 158° W
MLD (m)	46	62	38	46	34	60	50	64	66	48
Chl *a* (mg m^{-2})	12.7	25.1	30.3	27.3	26.8	31.9	33.0	24.4	18.2	13.2
Fucoxanthin (mg m^{-2})	0.6	2.7	2.0	2.7	1.4	2.4	4.9	2.6	1.2	0.4
Fuco:Chl *a*	0.05	0.11	0.07	0.10	0.05	0.08	0.15	0.11	0.07	0.03
N+N (μmol N m^{-2})	145	223	179	1347	708	274	285	218	75	205
SRP (μmol P m^{-2})	3406	3001	3986	3801	3679	2804	2164	2252	2223	1850
Si $(OH)_4$ (mmol Si m^{-2})	101	65	69	57	79	57	60	61	65	135
N+N:SRP (mol:mol)	0.04	0.07	0.05	0.35	0.19	0.10	0.13	0.10	0.03	0.11
SRP:Si $(OH)_4$ (mol:mol)	0.03	0.05	0.06	0.07	0.05	0.05	0.04	0.04	0.03	0.01

Abbreviations: Chl *a*, chlorophyll *a*; Fuco, fucoxanthin; MLD, mixed layer depth; N+N, $NO_3^- + NO_2^-$; SRP, soluble reactive phosphorus.

images obtained from the NASA Level 3 browser (http://oceancolor.gsfc.nasa.gov/cgi/level3.pl). Satellite sea level anomaly (SLA) images were obtained using the Global Near-Real Time Altimetry Data Viewer available from the Colorado Center for Astrodynamics Research (http://argo.colorado.edu/~realtime/gsfc_global-real-time_ssh/). The SLA back trajectory analyses step backward in time, locating the highest SLA closest to the previous position of the center of the eddy. The resulting trajectory analyses were consistent with Chelton *et al.* (2007).

Shipboard sampling for this study was conducted along a transect that bisected the observed center of the region of enhanced chlorophyll to the northwestern edge of the feature. Station locations were chosen based on 8-day composites of MODIS satellite-derived ocean color. Eleven stations were occupied during this transect, spanning a total distance of ~100 km (Table 1). The first several stations were spaced ~18 km apart, followed by several stations spaced ~9 km apart. Fluorescence profiles of chloropigment, equal to chlorophyll *a* plus phaeopigments, in the upper ocean (0–200 m) were measured using a SeaPoint fluorometer on a SeaBird conductivity–temperature–depth (CTD) system; fluorescence was calibrated with bottle chlorophyll measurements.

Water samples for subsequent DNA and RNA extractions were collected from four depths (5, 25, 45 and 100 m) using 12 l polyvinyl chloride bottles attached to the CTD rosette sampler. Additional water samples for biogeochemical measurements were collected from the same depths plus one additional depth (125 m) using the same CTD sampling bottles. These measurements included nutrients (N + N, SRP and silicic acid), fluorometric chlorophyll *a* and high-performance liquid chromatography pigments.

Biogeochemical analyses

Concentrations of chlorophyll *a* and phaeopigments (together termed chloropigments) were determined fluorometrically as described in Karl *et al.* (2001). Briefly, 125 ml subsamples of seawater were filtered onto Whatman 25 mm glass fiber filters, and extracted in 90% acetone in the dark at −20 °C for 7 days. Extracts were allowed to equilibrate to room temperature prior to measuring chlorophyll *a* and phaeopigment concentrations using a Turner AU-10 fluorometer. In addition, chlorophyll *a* and fucoxanthin concentrations were determined by high-performance liquid chromatography as described in Andersen *et al.* (1996). Two liters of seawater were filtered through 25 mm Whatman glass fiber filters, and the filters were placed in 2 ml cryovials (Corning) and flash frozen in liquid nitrogen. Upon return to the shore-based laboratory, filters were extracted in 100% acetone and pigments were analyzed by high-performance liquid chromatography.

N + N concentrations were measured using the high-sensitivity chemiluminescent analysis described by Garside (1982) as modified by Dore and Karl (1996). The precision of this method at concentrations $<50\,nmol\,l^{-1}$ averages $0.5\,nmol\,l^{-1}$ (Dore and Karl, 1996). SRP concentrations were measured using the MAGnesium-Induced Co-precipitation (MAGIC) method described by Karl and Tien (1992); the detection limit for SRP is 2–3 $nmol\,l^{-1}$, with an average precision of 5% for samples $<50\,nmol\,l^{-1}$. Silicic acid concentrations were measured spectrophotometrically using the molybdenum blue assay and a 10-cm cell as described in Strickland and Parsons (1972). The detection limit for the silicic acid assay is $\sim100\,nmol\,l^{-1}$.

Rates of N_2 fixation were measured from discrete water samples collected at 5 m depth using the assimilation of ^{15}N-labelled N_2 gas (Montoya *et al.*, 1996). Four and a half-liter polycarbonate bottles were overfilled with whole seawater, fitted with septum caps, and spiked with 3 ml of 98% $^{15}N_2$ and placed in an incubator plumbed with surface seawater shaded to 30% incident irradiance. After incubating for 24 h, samples were pressure filtered onto pre-combusted 25 mm glass fiber filters, dried and the ^{15}N isotope enrichment of particulate material was analyzed on an elemental analyzer–isotope ratio mass spectrometer (EA-IRMS Carlo Erba NC2500 coupled to a Thermo-Finnigan Delta S). Glycine was used as a standard for all samples and reproducibility was approximately 0.2 ‰ $\delta^{15}N$. Rates of N_2 fixation were calculated as described in Capone and Montoya (2001).

Nucleic acid collection and extraction

Whole seawater samples were subsampled into 2 l, acid-rinsed, polycarbonate bottles and 1–2 l were filtered through 25 mm, 0.22 μm pore size Durapore filters (Millipore, Billerica, MA, USA). Filters for DNA extractions were stored in 1.5 ml microcentrifuge tubes containing 500 μl of Tris-EDTA buffer and 0.2 g of autoclaved 0.1 mm zircon beads (Biospec Products Inc., Bartlesville, OK, USA). Filters to be used for RNA extraction were stored in microcentrifuge tubes containing 1% β-mercaptoethanol in RLT buffer (Qiagen RNeasy Kit) and 0.2 g of autoclaved 0.1 mm zircon beads (Biospec Products Inc.) Microcentrifuge tubes containing the filters were immediately quick frozen in liquid nitrogen and stored at −80 °C until extraction.

In the shore-based laboratory, the microcentrifuge tubes were agitated in a Fast Prep bead-beater machine (Bio 101) for a total of 1.5 min. DNA was extracted from the filters as described by Church *et al.* (2005a). DNA extracts were purified using the Qiagen DNeasy Kit following the manufacturer's protocols and stored at −20 °C. RNA samples were extracted following the methods described in Church *et al.* (2005b) using the Qiagen RNeasy Mini Kit (Cat. 74104, Qiagen, Valencia, CA, USA) following the manufacturer's instructions. Extracted RNA was stored at −80 °C until analysis.

Degenerate RT-PCR, cloning and sequencing

RNA extracts were reverse transcribed (RT) and PCR-amplified in a nested PCR reaction using degenerate primers as described in Zehr and Turner (2001). Reactions without RT were run simultaneously to verify amplification derived from mRNA. The resultant PCR products were visualized, cloned and sequenced as described by Zehr and Turner (2001). Sequences were edited using BioEdit Sequence Alignment Editor software (Hall, 1999), and the DNA sequences were imported into an aligned ARB sequence database for construction of neighbor-joining phylogenetic trees. Distances were determined using a Jukes–Cantor correction. Sequences with >94% similar identity were grouped into *nifH* phylotype clusters. The *nifH*-like *frxC* gene of *Plectonema boryanum* was used as an out-group to root the tree.

QPCR amplification of nifH phylotypes

Specific clusters of *nifH* containing sequences, derived from the PCR clone libraries, were targeted by quantitative PCR (QPCR) using specific primers and probes described in Church *et al.* (2005a, 2008). Seven sets of primers and probes were used to amplify specific *nifH* genes from the DNA extracts. These primer/probe sets targeted Groups A and B unicellular cyanobacteria; three groups of heterocystous cyanobacteria (termed Het_1, Het_2, and Het_3); *Trichodesmium* spp. and a group of *nifH* sequences phylogenetically related to proteobacteria (termed proteo_1). QPCR reactions were run in duplicate. The detection limit of the QPCR reaction corresponded to approximately 1 *nifH* gene copy per PCR reaction, equivalent to approximately 50–100 gene copies per l of seawater, depending on the volume of seawater filtered.

Results

Satellite-derived sea surface altimetry and pigment concentrations

In mid-July 2005, satellite observations of ocean color and sea surface altimetry revealed a $\sim35\,000\,km^2$ region of elevated SLA and enhanced chlorophyll located between 21° 45′ N, 156° 20′ W and 22° 45′ N, 158° 30′ W (Figure 1). Model-derived current vectors, which also assimilate observational data, showed clockwise circulation indicative of an anticyclone (http://www7320.nrlssc.navy.mil/global_ncom/plots/haw/). Hindsight reconstruction of the time and space trajectory of the eddy suggested that the anticyclone formed near 24°N, 138°W as early as April 2004 (Figure 2). The

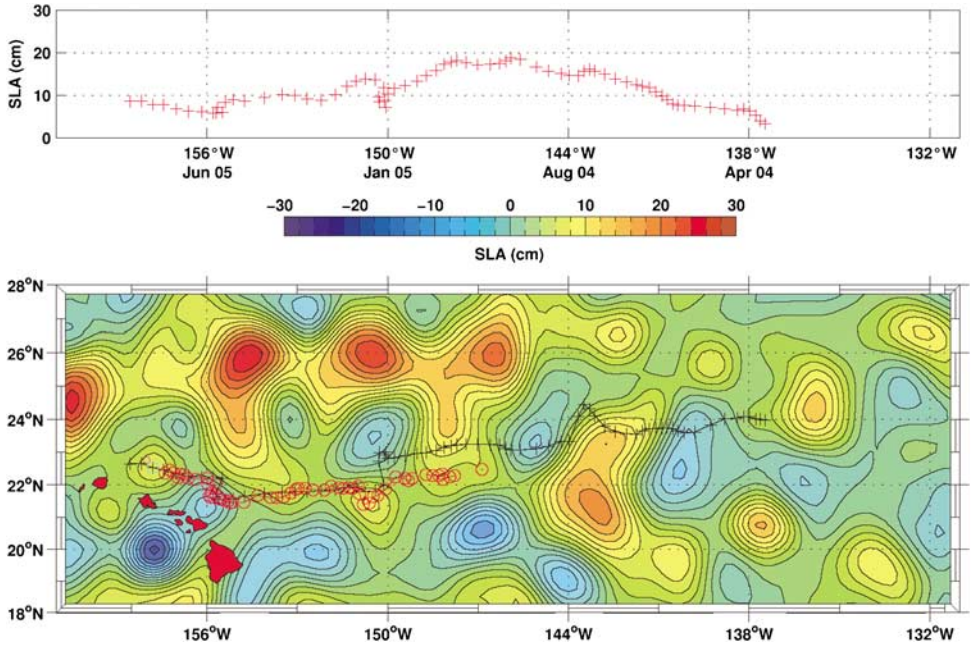


Figure 2 The history of the SLA for the center of the eddy plotted against longitude with the approximate time that the eddy center was located at a particular longitude (upper panel). The SLA map from the week of July 22nd based on the AVISO merged altimetry product (lower panel; Le Traon and Dibarboure, 1999). Superimposed on the map are back trajectory analyses depicting the history of the center of the anticyclone; red circles are based on a subjective analysis and black crosses depict an automated analysis. The size of the circles does not correspond to the eddy diameter. A cyan box surrounds the center of the eddy for the period represented by the map. The magenta circle nearby represents the area of Station ALOHA. SLA, sea level anomaly.

anticyclone appeared to intensify through 2004, attaining maximum SLA of ~20 cm in December 2004 (Figure 2). As the eddy matured and propagated westward, SLA gradually declined; in mid-June 2005, following a brief interaction with the northern slope of the island of Maui, the anticyclone intensified slightly (as reflected by increased SLA) before dissipating in early August. Ocean color satellite imagery revealed no discernable changes in near-surface chlorophyll associated with the eddy until early to mid-July; however, by July 20, sea surface chlorophyll concentrations associated with the eddy were four- to fivefold greater than the surrounding waters (concentrations in the eddy ranged 0.20–0.40 $\mu g\,l^{-1}$). By early August (6 August 2005), satellite altimetry indicated nearly complete dissipation of the eddy, while ocean color imagery suggested continued enhancement of sea surface chlorophyll until the middle of August 2005 (approximately 14 August 2005).

Shipboard sampling of the anticyclone provided an opportunity to examine depth-dependent variability in upper ocean biogeochemistry, N_2 fixation and diazotroph community structure. Vertical profiles of potential density (calculated from measurements of temperature and salinity) along the eddy transect revealed upper mixed layer depths varied between ~34 and 66 m (Table 1), with generally deeper mixing at those stations near the leading edge of the eddy (Figure 3). These patterns may reflect stronger vertical shear of horizontal flow with associated enhancement in upper ocean mixing along the periphery of the eddy. Spatial variability in the physical structure of the eddy appeared to influence resulting biological responses. In particular, vertical profiles of fluorescence revealed that chloropigment concentrations were highly variable within the eddy, with peak concentrations typically occurring near the base of the mixed layer (Figure 4). Moreover, vertical distributions of N + N and chloropigment within the anticyclone differed from those sampled outside the eddy during HOT cruises immediately prior to (HOT 171) and following (HOT 172) the passage of the eddy over Station ALOHA. Concentrations of N + N were elevated in the lower regions of the euphotic zone compared to HOT cruises 171 and 172, and peak chlorophyll concentrations were shifted upwards relative to those observed on HOT 171 or 172. Examination of the chloropigment concentrations along isopycnal surfaces revealed this redistribution and enhancement of upper ocean chlorophyll was not the result of an upward displacement of the deep chlorophyll maximum. In general, chlorophyll *a* inventories (0–100 m) were two- to threefold greater than typically observed at Station ALOHA (Figure 5a, Table 1), with peak inventories greater at mid-transect stations than along the leading edge or outside of the eddy (Table 1).

Depth profiles of fucoxanthin, an accessory pigment produced by diatoms, revealed increased concentrations and vertical redistribution of this pigment relative to HOT 171 and 172 (Figure 4, Table 1). Depth integrated (0–100 m) inventories of

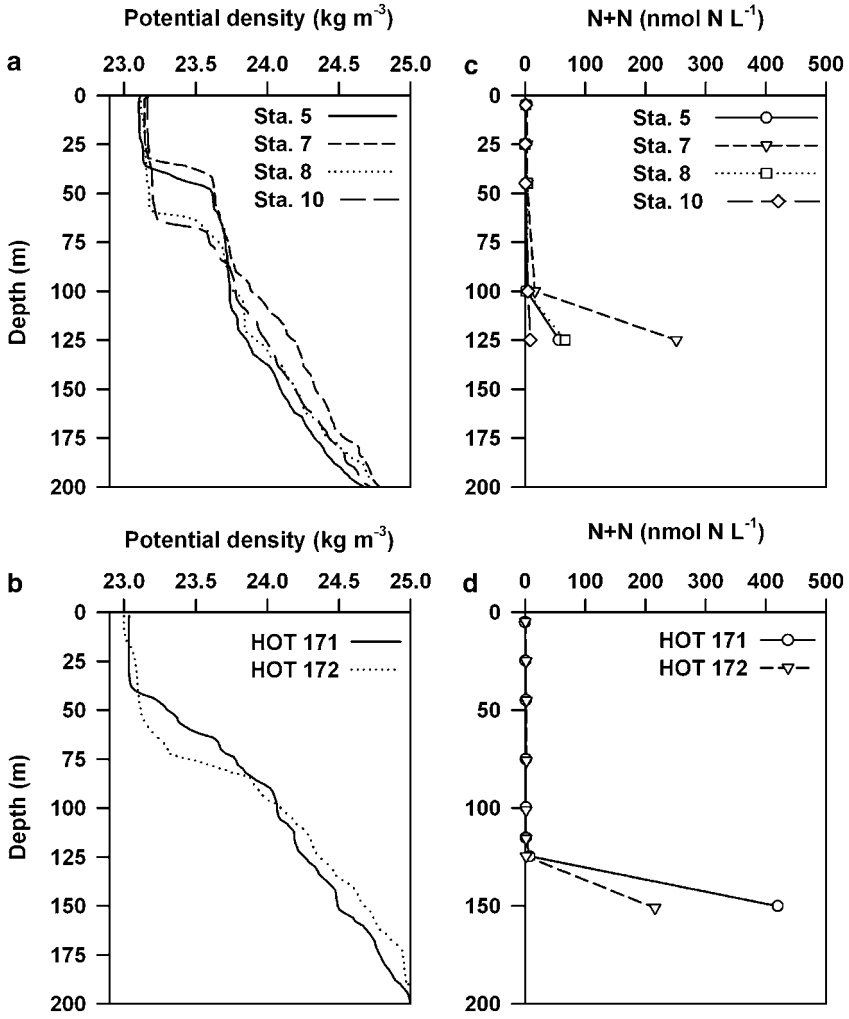


Figure 3 Vertical profiles of potential density (**a**, **b**) and N + N (**c**, **d**) from selected stations along the eddy transect (top panels) and at Station ALOHA (bottom panels). Station positions are provided in Table 1; Sta. 5 was near the eddy center, while Sta. 10 was near the leading edge of the eddy. Profiles from HOT cruises depict vertical distributions and concentrations immediately preceding (HOT 171) and following (HOT 172) the passage of the eddy over Station ALOHA.

fucoxanthin in the eddy were ~2–4 fold greater than those typically observed at Station ALOHA (Figure 5b). Moreover, fucoxanthin inventories were two- to fourfold greater than measured on cruises immediately before and after the passage of the eddy (Table 1). The ratio of fucoxanthin: chlorophyll *a* in the near-surface waters (used to identify the relative contribution of diatoms to total chlorophyll *a*) peaked along the leading edge of the eddy, where rates of N_2 fixation were elevated (Figure 6).

Nutrient concentrations and inventories

Within the anticyclone, concentrations of N + N were consistently low, but variable in space; near-surface water concentrations of N + N ranged 0.5–3 nmol l^{-1}. Near-surface ocean concentrations of SRP ranged from 12 to 19 nmol l^{-1}; these SRP concentrations are on the lower end of the ~18 year record measured at Station ALOHA; however, the depth integrated inventories (0–100 m) of SRP were not significantly different (one-way analysis of variance, $P<0.05$) from the ALOHA summertime climatology (Figure 5). On the HOT cruise immediately following passage of the eddy, inventories of SRP were up to twofold lower than concentrations observed within the eddy (Table 1). The N + N: SRP ratio in the near-surface waters of the eddy ranged between 0.03 and 0.22, peaking in the mid regions of the transect (Figure 6). In contrast, upper ocean silicic acid concentrations and inventories (0–100 m) were significantly lower (by two- to threefold) than the seasonal climatology for this region (Figure 5d, Table 1).

Nitrogen fixation rates and RT-PCR clone library

Near-surface (5 m) ocean rates of N_2 fixation demonstrated considerable spatial variability ranging from 4.4 to 22.8 nmol N per l per day (Figure 6). In general, rates of N_2 fixation tended to increase toward the leading edge of the eddy (Figure 6);

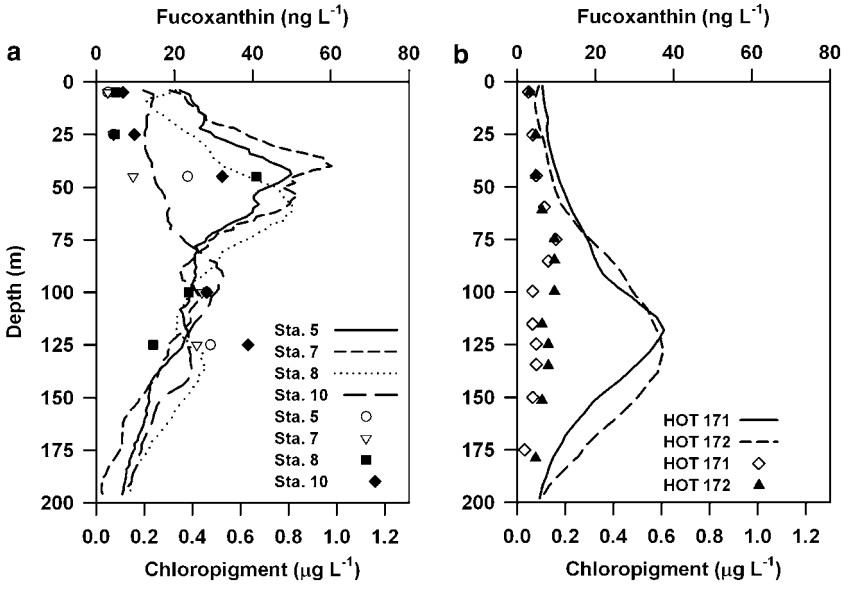


Figure 4 Vertical profiles of chloropigment and fucoxanthin concentrations from stations within the eddy (**a**) and during HOT cruises preceding and following passage of the eddy (**b**).

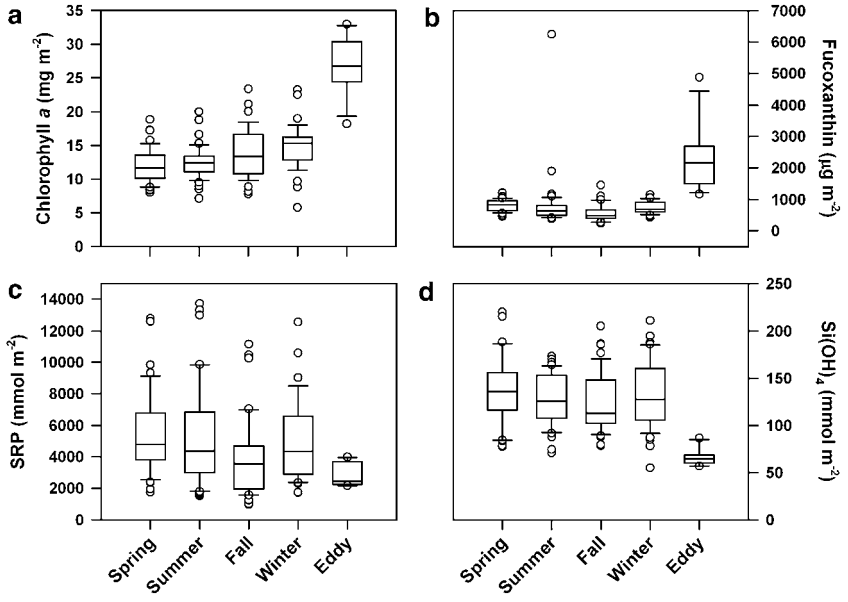


Figure 5 Depth-integrated (0–100 m) seasonal inventories of pigments and nutrients measured at Station ALOHA (1989–2005) compared to pigments and nutrient inventories within the eddy. The lower bound of the box represents the lower quartile, the line within the box represents the median and the upper bound of the box represents the 75% quartile. The open circles represent outliers in the data; (**a**) chlorophyll *a*; (**b**) fucoxanthin; (**c**) SRP and (**d**) silicic acid. SRP, soluble reactive phosphorus.

however, the large spatial variability observed in rates of N_2 fixation made it difficult to discern whether this spatial asymmetry was real or derived from low sampling resolution within the feature.

In total, 177 clones from RT-PCR amplified *nifH* transcripts were sequenced as part of this study (Figure 7). Seven groups of sequences were identified including five phylotypes that clustered among previously identified *nifH* containing cyanobacteria (Zehr *et al.*, 2001; Church *et al.*, 2005b) and two phylotypes that clustered among *nifH* containing proteobacteria, including one novel sequence type that clustered among proteobacteria *nifH* sequences. Filamentous cyanobacterial sequences dominated the *nifH* RT-PCR clone library (Figure 7); approximately 71% (126 sequences) of the sequences clustered closely (>98% identity) with *nifH* genes from *Katagnymene spiralis* and *Trichodesmium* spp., while ~8% (14 sequences) of the sequences clustered among previously described heterocyst-forming cyanobacteria (Figure 7). Sequences clustering among unicellular *nifH* containing cyanobacteria comprised ~8% (15 sequences) of the RT-PCR clone library, including phylotypes

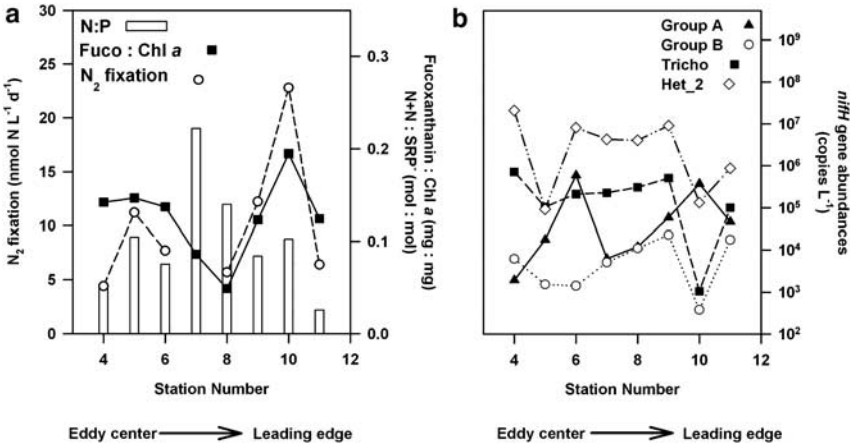


Figure 6 Near-surface ocean (5 m) (**a**) rates of N_2 fixation, N + N:SRP ratios and fucoxanthin:chlorophyll *a* ratios sampled along the eddy cruise transect and (**b**) gene copy abundances of several of the prominent *nifH*-containing cyanobacteria examined in this study. Station positions are indicated in Table 1; station 4 was located near the center of the eddy, station 11 along the western (leading) edge of the eddy. SRP, soluble reactive phosphorus.

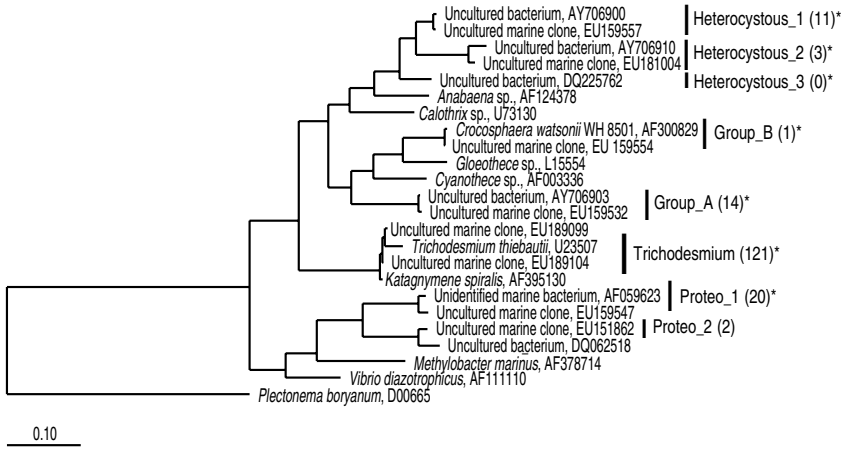


Figure 7 Neighbor-joining phylogenetic tree depicting relationships of *nifH* sequences. Sequences sharing 94% identity were grouped and these groupings are shown in bold. Groups targeted for QPCR are denoted by an asterisk. Accession numbers for representative sequences for each group are shown in parentheses. QPCR, quantitative PCR.

identical to *Crocosphaera watsonii* (termed Group B) and the previously described Group A cyanobacteria. Twenty-two sequences clustered among *nifH* containing proteobacteria with the majority of these sequences (20) clustering with a previously described proteobacterial *nifH* phylotype (termed proteo_1) and two sequences forming a distinct group of sequences termed proteo_2 (Figure 7).

Vertical distribution of diazotrophs

Quantitative PCR amplification of several of the *nifH* phylotypes retrieved from the RT-PCR clone libraries revealed considerable variability in the both the distributions and abundances of N_2 fixing microorganisms within the eddy (Figure 8). In general, heterocyst-forming cyanobacteria, in particular, a phylotype-termed Heterocystous_2 (Het_2), had the greatest *nifH* gene copy abundances of the groups examined (Figure 8); however, the abundances of these phylotypes were highly variable in space (both vertically and along the sampling transect; Figures 5 and 7). The abundances of the Het_2 phylotype were two to three orders of magnitude greater than the other heterocystous cyanobacteria phylotypes examined (Figure 8b). The Het_2 phylotype displayed elevated abundances in the near-surface waters, ranging from 10^6 to 10^7 gene copies per l, and declining approximately two orders of magnitude with depth. On average, gene copy abundances of the other heterocystous phylotypes (termed Het_1 and Het_3, respectively) examined by QPCR were nearly three orders of magnitude lower than the Het_2 phylotype, with near-surface water abundances of Het_1 and Het_3 averaging $\sim 10^4$ gene copies per l

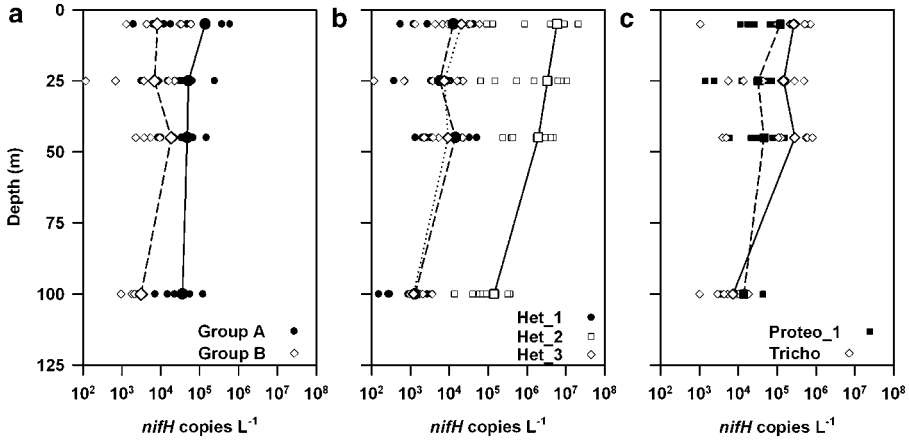


Figure 8 Depth distributions (all stations) of *nifH* containing bacteria determined by QPCR. (**a**) Average gene copy abundance of Groups A and B unicellular *nifH* phylotype; solid line depicts mean concentrations of Group A for all stations, dashed line depicts mean Group B abundances. (**b**) Depth distributions (all stations) of heterocystous phylotypes; dashed line depicts mean Het_1 phylotype abundances, solid line depicts mean Het_2 abundances and dotted line depicts average Het_3 phylotype copy abundances. (**c**) Depth distributions (all stations) of gene copy abundance of *Trichodesmium* and proteobacteria; solid line depicts abundances of Tricho phylotype, dashed line depicts average proteo_1 phylotype abundances. QPCR, quantitative PCR.

Table 2 Summary of depth-integrated (0–100 m) *nifH* gene copies (copies per m^2) at stations sampled within the anticyclonic eddy and during HOT cruises immediately before and following passage of the eddy over Station ALOHA

nifH copies m^{-2}	*HOT 171*	*Station 4*	*Station 5*	*Station 6*	*Station 7*	*Station 8*	*Station 9*	*Station 10*	*Station 11*	*HOT 172*
Unicells	6.6×10^9	8.1×10^9	1.4×10^9	9.2×10^9	6.8×10^9	5.6×10^9	5.8×10^9	9.4×10^9	5.2×10^9	1.9×10^9
Group A	6.4×10^9	5.8×10^9	1.3×10^9	7.4×10^9	6.4×10^9	5.4×10^9	4.6×10^9	6.7×10^9	4.1×10^9	1.7×10^9
Group B	2.6×10^8	2.3×10^9	6.1×10^7	1.9×10^9	4.0×10^8	1.9×10^8	1.2×10^9	2.8×10^9	1.1×10^9	1.5×10^8
Heterocyst-forming	7.2×10^9	4.4×10^{11}	3.5×10^9	4.2×10^{11}	1.9×10^{11}	1.9×10^{11}	2.5×10^{11}	1.3×10^{11}	3.9×10^{10}	2.2×10^9
Het_1	1.1×10^8	5.2×10^8	1.3×10^7	2.5×10^8	2.9×10^8	2.0×10^8	1.8×10^9	2.1×10^9	1.3×10^9	2.3×10^7
Het_2	6.7×10^9	4.3×10^{11}	3.3×10^9	4.2×10^{11}	1.9×10^{11}	1.9×10^{11}	2.5×10^{11}	1.2×10^{11}	3.6×10^{10}	1.4×10^9
Het_3	3.2×10^8	8.1×10^8	1.5×10^8	3.7×10^8	8.7×10^8	3.0×10^8	1.4×10^9	N/D	1.3×10^9	8.1×10^8
Trichodesmium	1.8×10^{10}	1.7×10^{10}	1.8×10^9	2.6×10^{10}	2.7×10^{10}	3.4×10^{10}	1.1×10^{10}	5.7×10^9	1.1×10^{10}	1.7×10^{10}
Proteobacteria	—	2.9×10^9	4.3×10^8	3.1×10^9	2.2×10^9	2.0×10^9	1.2×10^{10}	4.5×10^9	4.1×10^9	—

Station locations provided in Table 1.
The subdivisions of the Unicells and Heterocyst-forming groups are shown in italics beneath the main heading. ND indicates phylotype below detection in this sample; — indicates no information on phylotype abundance for this cruise.

(Figure 8b). Among the unicellular cyanobacteria, average gene copy abundances of the presumed unicellular Group A phylotype were approximately an order of magnitude greater than the Group B phylotype (Figure 8a). The abundances of the unicellular phylotypes within the eddy were also highly variable in space. Near the leading edge of the eddy where rates of N_2 fixation were highest (Station 10) *nifH* gene copy abundances of the Group A phylotype were greater in the near-surface water than any of the other phylotypes examined. Gene copy abundances of *Trichodesmium* were consistently elevated (generally $>10^5$ *nifH* gene copies per l) in the well-lit regions of the upper ocean, declining approximately an order of magnitude by 100 m (Figure 8c). On average, gene copy abundances of the proteo_1 phylotype were similar to *Trichodesmium* and the Group A phylotypes; distributions of the proteo_1 phylotype were fairly constant throughout the upper 100 m (ranging between 10^4 and 10^5 gene copies per l) (Figure 8c).

Depth-integrated nifH *gene inventories*

Heterocystous cyanobacteria, specifically the Het_2 phylotype, dominated the depth-integrated (0–100 m) *nifH* copy inventories along the eddy transect (Table 2). At several stations, the combined abundances of the heterocystous phylotypes were more than two orders of magnitude greater than those sampled at Station ALOHA before and after the eddy transect cruise. Copy abundances of the heterocystous cyanobacteria ranged between $\sim10^8$ and 10^{11} copies per m^2. However, the abundances of the heterocystous phylotypes was highly variable in space; depth integrated (0–100 m) gene copies of Het_1, Het_2 and Het_3 groups varied six-, seven- and fivefold between stations, respectively (Table 2).

Among the unicellular cyanobacterial phylotypes, the Group A phylotype was the most abundant (Figure 8), and both the Groups A and B *nifH* gene inventories were less spatially variable (ranging ~2-fold) than filamentous *nifH* phylotypes. The unicellular Group B phylotype demonstrated considerable variability in space and time; abundances were nearly an order of magnitude greater at selected stations (4, 6, 10, 11) relative to inventories measured before and after the passage of the eddy (Table 2).

Trichodesmium accounted for $\sim 10^{10}$ gene copies per m^2, often exceeding inventories of the Het_1, Het_3, both groups of unicellular cyanobacteria and proteobacteria. *Trichodesmium nifH* gene inventories peaked in the middle of the sampling transect coincident with the region of enhanced chlorophyll. In comparison to cruises sampled before and after the eddy, *Trichodesmium* gene inventories demonstrated only modest increase (two- to threefold; Table 2). Depth-integrated proteobacteria *nifH* gene inventories were generally greatest along the leading edge (western-side) of the eddy (Table 2, Station 11), averaging $\sim 10^9$ copies per m^2.

Discussion

Biological productivity and plankton biomass in the upper ocean of the oligotrophic North Pacific Ocean demonstrate temporal and spatial variability (Venrick, 1993; Karl, 1999). Use of remote sensing technologies has revealed considerable mesoscale variability in physical and bio-optical parameters throughout the open ocean gyres. By combining satellite altimetry and ocean color determinations with a shipboard sampling opportunity, we assessed the spatial structure of diazotroph assemblages associated with a mesoscale anticyclonic eddy near Station ALOHA. Back trajectory analyses of the anticyclone suggested that at the time of our sampling (26 July 2005), the anticyclonic eddy was dissipating (Figure 2). Despite relatively weak positive SLA anomalies at the time of sampling, a shipboard Acoustic Doppler Current Profiler confirmed apparent clockwise circulation within the feature, consistent with an anticyclone. Such observations would suggest downwelling of isopycnal surfaces would accompany this eddy; however, our shipboard transect of the eddy revealed that mixed layer depths generally shoaled near the center of the eddy, suggesting that isopycnal surfaces may have relaxed as the eddy dissipated.

Satellite-derived estimates of sea surface chlorophyll revealed a clear biological response during the waning stages of the eddy. The spatial distribution of chloropigment sampled along a transect through the eddy indicated that one of the prominent biological responses to this eddy was an enhancement and redistribution of photosynthetic biomass in the upper ocean. Within the central regions of the eddy, chloropigment concentrations displayed shallow subsurface maxima (25–80 m), typically peaking near the base of the mixed layer. In contrast, chloropigment concentrations at Station ALOHA are generally elevated deep in the euphotic zone (125 ± 9 m), approximately coincident with the top of the nitracline (Letelier *et al.*, 2004). The anticyclonic eddy appeared to enhance photoautotrophic biomass; chlorophyll *a* inventories (0–100 m) were approximately two times greater than the summertime climatology at Station ALOHA. Depth-integrated inventories of N + N were similar to the summertime distributions measured at Station ALOHA; however, inventories of SRP and silicic acid were both lower than typically measured at Station ALOHA. The apparent de-coupling of SRP and Si from N + N pools is consistent with the measured enhancement of N_2 fixation, elevated abundances of N_2 fixing microorganisms and increased diatom biomass observed within the eddy. The similarity in N + N inventories and dissimilarity of SRP and silicic acid inventories suggest an uncoupling in the uptake or input of N relative to P and Si. Increased inorganic nutrient N:P ratios support the observation that diazotrophs dominated the plankton assemblage at the time of this study, while the decreased availability of silicic acid and enhanced concentrations of fucoxanthin are consistent with epifluorescence microscopy-based observations, which revealed that several diatoms, including *Rhizosolenia* spp., *Hemiaulus* spp. and *Chaetoceros* spp. were abundant within the eddy.

One of the primary objectives of our sampling of this mesoscale feature was to examine spatial variations in rates of N_2 fixation and the abundances of N_2 fixing microorganisms. Within the anticyclone, measurements of upper ocean rates of N_2 fixation were greater than those previously reported for this region of the North Pacific. Previous studies have described seasonal increases in N_2 fixation at Station ALOHA; these studies indicate rates typically peak in the summer when the upper ocean is stratified and light fluxes are high. Previous reports of near-surface ocean rates of N_2 fixation at Station ALOHA range from 0.9 to 1.68 nmol N per l per day (Dore *et al.*, 2002; Grabowski *et al.*, in review); in the present study, rates within the eddy were ~2–18 times greater than these previous measurements. These results suggest that mesoscale processes introduce variability to seasonal fluctuations in N_2 fixation and diazotroph community structure in the NPSG.

We also examined the diversity and distributions of N_2 fixing bacteria within the eddy based on RT-PCR amplification of *nifH* gene transcripts and QPCR amplification of *nifH* genes. RT-PCR clone libraries revealed a majority of *nifH* sequences clustered with previously identified phylotypes. The majority (71%) of sequences were >98% identical to *nifH* sequences of *Trichodesmium* spp. The remaining sequences clustered with previously

described unicellular cyanobacteria (Groups A and B), heterocyst-forming cyanobacteria (termed Het_1, Het_2 and Het_3) and proteobacteria (Zehr *et al.*, 1998; Church *et al.*, 2005b; Foster and Zehr, 2006). Nitrogenase gene expression has been shown to demonstrate light–dark dependence in various cyanobacteria, including *Trichodesmium* spp., and *nifH* transcription patterns appear highly dependent on diel phasing (Ohki *et al.*, 1992; Zehr *et al.*, 1993; Wyman *et al.*, 1996; Chen *et al.*, 1998; Church *et al.*, 2005b). Our sampling of the eddy was largely restricted to pre-dawn hours, a time when *nifH* expression by *Trichodesmium* spp. would likely be elevated, perhaps explaining the dominance of *Trichodesmium* spp. phylotypes in our RT-PCR amplified *nifH* clone libraries. In contrast, the Group B *nifH* phylotype demonstrates peak expression at night (Church *et al.*, 2005b), again possibly accounting for the low transcript abundances from this phylotype recovered in our study.

Two of the 177 clones that were sequenced formed a distinct phylotype among *nifH* containing proteobacteria (termed proteo_2); this phylotype was less than 95% similar to previously identified *nifH* containing proteobacteria. The QPCR-derived inventories of proteobacteria-like *nifH* copies from this study were as great as the inventories of the unicellular cyanobacteria and some of the heterocystous phylotypes, suggesting that these *nifH* phylotypes may comprise a large fraction of the *nifH* containing plankton.

Within the eddy, QPCR amplification revealed that heterocystous cyanobacteria were a highly variable, but generally abundant component of the diazotroph community. In comparison to the depth integrated *nifH* abundances sampled immediately prior to (HOT 171) and following (HOT 172) the passage of this eddy over Station ALOHA, abundances of the heterocystous cyanobacteria (specifically the Het_2 phylotype) appeared most influenced by this eddy. Previous studies have documented observations of diatom–cyanobacteria symbioses and more recent data combining molecular techniques with epifluorescence microscopy have constrained host specificity among diatoms and their cyanobacterial symbionts (Janson *et al.*, 1999; Carpenter, 2002; Foster and Zehr, 2006). These studies have shown that the filamentous heterocystous cyanobacterium, *Richelia intracellularis* appears associated with the planktonic diatoms *Rhizosolenia clevei* and *Hemiaulus hauckii*. Comparisons of the *hetR* gene, *nifH* gene and 16S rRNA sequences of heterocyst-forming cyanobacteria showed that the *nifH* sequences deriving from the Het_1 phylotype belong to symbionts of *R. clevei*, the Het_2 sequence type appears to derive from *R. intracellularis* that associates with *H. hauckii*, while the Het_3 sequence type is nearly identical to the epibiont *Calothrix* sp. often found associated with *Chaetoceros* sp. (Foster and Zehr, 2006). Consistent with these observations, examination of samples collected during the eddy cruise transect by epifluorescence microscopy revealed heterocyst-forming cyanobacteria as epi-symbionts and/or endosymbionts of large diatoms, including *Hemiaulus* spp., *Rhizosolenia* spp. and *Chaetoceros* spp.

In addition to increased abundances of heterocystous cyanobacteria within the eddy, RT-PCR clone library results and QPCR-derived abundances suggest that the anticyclone favored the growth of *Trichodesmium* and unicellular diazotrophs. Groups A and B *nifH* copies at Station ALOHA have been reported to range between 10^2 and 10^5 copies per l (Church *et al.*, 2005a), while abundances of these groups in the present study varied between 10^4 and 10^5 copies per l. In an $\sim$3 year study (1989–1992) at Station ALOHA, Letelier and Karl (1996) estimated of *Trichodesmium* abundances ranged between 10^3 and 10^4 cells per l; in the present study, *Trichodesmium* gene copies exceeded 10^5 copies per l in the near-surface waters and remained elevated throughout the upper ocean. During a large *Trichodesmium* bloom in the summer of 1989 at Station ALOHA, Karl *et al.* (1992) reported *Trichodesmium* abundances of upward of 10^8 cells per l. Assuming each *Trichodesmium* cell contains a single *nifH* gene copy, the abundances sampled during the present study were not as great as those observed in the bloom of 1989. However, *nifH* copy abundances of the heterocystous cyanobacteria appear to have rivaled *Trichodesmium* abundances observed during the 1989 bloom. It is important to note that several heterocystous cyanobacteria, including *Anabaena variabilis* and *Fischerella* sp., contain multiple *nifH* genes; furthermore, only the heterocyst is active in N_2 fixation, but both vegetative cells and heterocysts would contribute to estimates of *nifH* gene copy abundances.

Together, these data suggest physical and biogeochemical processes associated with the decaying anticyclone enhanced the growth of several groups of diazotrophs. Such observations are consistent with previous determinations of the mesoscale distributions of *Trichodesmium*; in a transect across the subtropical and tropical Atlantic Ocean, Davis and McGillicuddy (2006) used a video plankton recorder to evaluate the distributions of *Trichodesmium*. These authors determined that *Trichodesmium* spp. abundances were consistently greater within anticylonic eddies relative to the surrounding waters. In the present study, molecular approaches revealed that several groups of N_2 fixing microorganisms, including *Trichodesmium* spp., were enhanced within the eddy relative to the surrounding waters.

There are a number of potential processes that could create conditions favorable to the growth of N_2 fixing microorganism within an anticylonic eddy. The downwelling structure of anticyclonic eddies vertically displace nutrient-enriched waters from the well-lit regions of the euphotic zone, potentially exacerbating already weak vertical exchange of nutrients observed in the NPSG. Such conditions

may have permitted slower growing N_2 fixing microorganisms to out compete (for light and nutrients) organisms dependent on vertical inputs of nutrients. Such a mechanism does not account for the sources of other bioessential nutrients, such as phosphorus, iron and silicic acid that would have been required to sustain the growth of N_2 fixing microbes and diatoms observed in the eddy. Another possibility is that high shear along the periphery of the eddy enhanced turbulent mixing and diapycnal nutrient exchange. Such edge-associated nutrient input has been observed in other anticyclonic features (Yentsch and Phinney, 1985). In the present study, we saw no clear enhancement of SRP or $N+N$ concentrations near the boundary of the eddy; however, rates of N_2 fixation and the relative contributions of diatoms to the photosynthetic community structure (as determined by the ratio of fucoxanthin:Chl *a*) increased toward the leading edge of the eddy. Another possibility is that the physically isolating eddy vorticity provided a means to transport exogenous flora from one of the oceanic regions bisected during the eddy's westward trajectory. However, the results of our clone libraries and QPCR enumeration of *nifH* gene abundances suggest that the N_2 fixing microorganisms were generally similar to those previously sampled at Station ALOHA, but that the relative abundances of several of these groups of organisms was enhanced, implying conditions within the eddy favored net growth of the resident diazotroph populations. Moreover, near-surface chlorophyll concentrations, as detected by the MODIS ocean color satellite suggest that the accompanying biological response occurred within the vicinity of Station ALOHA.

Perhaps the most intriguing possible mechanism relates to deformation of isopycnal surfaces as the eddy matured and intersected the Hawaiian Islands. Dissipation of the eddy may have relaxed isopycnal surfaces, reintroducing nutrient-enriched waters to the euphotic zone. Vertical profiles of potential density indicated possible relaxation of isopycnal surfaces toward the central regions of the eddy. This potential relaxation may have been facilitated by a presumed interaction of the eddy with the northern slope of Maui. The SLA back trajectory analyses suggest that the southern edge of the eddy impinged on the northern slope of Maui in early June; this interaction appears to have partly facilitated the eddy decay. Evaluation of the satellite chlorophyll response indicates that if some interaction with Maui influenced the physics or biogeochemistry of the eddy, the accompanying biological response was notable approximately 1 month later. Regardless of the mechanism(s), taken as a whole, our observations point to an important new role that eddies might play in enhancing ocean production not only in upwelling (cyclonic) eddies through nutrient pumping but also in downwelling (anticyclonic) eddies via promotion of diazotroph growth.

The physical and biological mechanisms supporting an increase of diazotrophy during such mesoscale events remain unknown. The MODIS derived chlorophyll field indicated that a large region north of Station ALOHA also displayed enhanced sea surface chlorophyll during our sampling of this eddy; this region was also associated with positive SLA. Such results suggest that mesoscale processes may enhance the seasonal response of diazotrophs in the near-surface waters of the NPSG. Further studies directed toward characterizing the microbial assemblage response to mesoscale perturbations during different seasons and water column conditions may help constrain the role of such event-scale forcing on N_2 fixation in the oligotrophic oceans.

Acknowledgements

The dedicated efforts of the staff of the Biogeochemical & Ecological Analyses of Complex Habitats (BEACH) lab were instrumental to this study. Special thanks to Patricia McAndrew and Dan Sadler for their sampling efforts at sea. Paul Lethaby and Fernando Santiago-Mandujano aided in the collection and analyses of the physical oceanographic and satellite altimetry data. The comments of Grieg Steward and two anonymous reviewers improved this paper. We thank Robert Weller for accommodating our sampling with his ship time support from a NOAA funded project. Funding to support this research derived from grants from the National Science Foundation, including OCE-0425363 to MJC and JPZ, OCE-0327513 to RL, and EF-0424599 (C-MORE) awarded to the University of Hawaii. Additional support was provided from Gordon and Betty Moore Foundation Investigator in Marine Microbiology awards to JPZ and DMK.

References

Allen CB, Kanda J, Laws EA. (1996). New production and photosynthetic rates within and outside a cyclonic mesoscale eddy in the North Pacific subtropical gyre. *Deep Sea Res I* **43**: 917–936.

Andersen RA, Bidigare RR, Keller MA, Latasa M. (1996). A comparison of HPLC pigment signatures and electron microscopic observations for oligotrophic waters of the North Atlantic and Pacific Oceans. *Deep Sea Res II* **43**: 517–537.

Capone DG, Burns JA, Montoya JP, Subramaniam A, Mahaffey C, Gunderson T *et al.* (2005). Nitrogen fixation by *Trichodesmium* spp.: an important source of new nitrogen to the tropical and subtropical North Atlantic Ocean. *Global Biogeochem Cycles* **19**: GB2024.

Capone DG, Montoya JP. (2001). Nitrogen fixation and denitrification. In: Paul JH (ed). *Methods in Microbiology*, Vol 30. Academic Press: San Diego, pp 501–515.

Carpenter E. (2002). Marine cyanobacterial symbioses. *Proc R Irish Acad* **102B**: 15–18.

Chelton DB, Schlax MG, Samelson RM, de Szoeke RA. (2007). Global observations of large oceanic eddies. *J Geophys Res* **34**: L15606.

Chen YB, Dominic B, Mellon MT, Zehr JP. (1998). Circadian rhythm of nitrogenase gene expression in the diazotrophic filamentous nonheterocystous cyanobacterium *Trichodesmium* sp strain IMS101. *J Bacteriol* **180**: 3598–3605.

Church MJ, Bjorkman KM, Saito MA, Karl DM, Zehr JP. (2008). Regional distributions of nitrogen fixing bacteria in the Pacific Ocean. *Limnol Oceanogr* **53**: 63–77.

Church MJ, Jenkins BD, Karl DM, Zehr JP. (2005a). Vertical distributions of nitrogen-fixing phylotypes at Station ALOHA in the oligotrophic North Pacific Ocean. *Aquat Microb Ecol* **38**: 3–14.

Church MJ, Short CM, Jenkins BD, Karl DM, Zehr JP. (2005b). Temporal patterns of nitrogenase (*nifH*) gene expression in the oligotrophic North Pacific Ocean. *Appl Environ Microbiol* **71**: 5362–5370.

Davis CS, McGillicuddy DJ. (2006). Transatlantic abundance of the N_2 fixing colonial cyanobacterium *Trichodesmium*. *Science* **312**: 1517–1520.

Deutsch C, Gruber N, Key RM, Sarmiento JL, Ganachaud A. (2001). Denitrification and N_2 fixation in the Pacific Ocean. *Global Biogeochem Cycles* **15**: 483–506.

Dore JE, Brum JR, Tupas LM, Karl DM. (2002). Seasonal and interannual variability in sources of nitrogen supporting export in the oligotrophic subtropical North Pacific Ocean. *Limnol Oceanogr* **47**: 1595–1607.

Dore JE, Karl DM. (1996). Nitrite distributions and dynamics at station ALOHA. *Deep Sea Res II* **43**: 385–402.

Falkowski PG, Ziemann D, Kolber Z, Bienfang PK. (1991). Role of eddy pumping in enhancing primary production in the ocean. *Nature* **352**: 55–58.

Foster RA, Zehr JP. (2006). Take care *nifH*, *hetR* and 16S rRNA sequence diversity in the symbiotic heterocystous cyanobacteria, *Richelia intracellularis* and *Calothrix rhizosoleniae*. *Environ Microbiol* **8**: 1913–1925.

Garside C. (1982). A chemi-luminescent technique for the determination of nanomolar concentrations of nitrate and nitrite in seawater. *Mar Chem* **11**: 159–167.

Gruber N, Sarmiento JL. (1997). Global patterns of marine nitrogen fixation and denitrification. *Global Biogeochem Cycles* **11**: 235–266.

Hall TA. (1999). BioEdit: a user-friendly biological sequence alignment editor and analysis program for Windows 95/98/NT. *Nucleic Acids Sympos Ser* **41**: 95–98.

Janson S, Wouters J, Bergman B, Carpenter EJ. (1999). Host specificity in the *Richelia*–diatom symbiosis revealed by *hetR* gene sequence analysis. *Environ Microbiol* **1**: 431–438.

Karl D, Letelier R, Tupas L, Dore J, Christian J, Hebel D. (1997). The role of nitrogen fixation in biogeochemical cycling in the subtropical North Pacific Ocean. *Nature* **388**: 533–538.

Karl DM. (1999). A sea of change: biogeochemical variability in the North Pacific Subtropical Gyre. *Ecosystems* **2**: 181–214.

Karl DM, Bjorkman KM, Dore JE, Fujieki L, Hebel DV, Houlihan T *et al.* (2001). Ecological nitrogen-to-phosphorus stoichiometry at station ALOHA. *Deep Sea Res II* **48**: 1529–1566.

Karl DM, Letelier RM, Hebel DV, Bird DF, Winn CD. (1992). *Trichodesmium* blooms and new nitrogen in the North Pacific Gyre. In: Carpenter EJ, Capone DG (eds). *Marine Pelagic Cyanobacteria: Trichodesmium and Other Diazotrophs*. Kluwer Academic Publishers: Dordrecht, The Netherlands, pp 219–237.

Karl DM, Tien G. (1992). MAGIC—a sensitive and precise method for measuring dissolved phosphorus in aquatic environments. *Limnol Oceanogr* **37**: 105–116.

Le Traon P-Y, Dibarboure G. (1999). Mesoscale mapping capabilities of multi-satellite altimeter missions. *J Atmos Oceanic Technol* **16**: 1208–1223.

Letelier RM, Karl DM. (1996). The role of *Trichodesmium* spp. In the productivity of the subtropical North Pacific Ocean. *Mar Ecol Prog Ser* **133**: 263–273.

Letelier RM, Karl DM, Abbott MR, Bidigare RR. (2004). Light driven seasonal patterns of chlorophyll and nitrate in the lower euphotic zone of the North Pacific Subtropical Gyre. *Limnol Oceanogr* **49**: 508–519.

Letelier RM, Karl DM, Abbott MR, Flament P, Freilich M, Lukas R *et al.* (2000). Role of late winter mesoscale events in the biogeochemical variability of the upper water column of the North Pacific Subtropical Gyre. *J Geophys Res Oceans* **105**: 28723–28739.

Lipschultz F, Owens NJP. (1996). An assessment of nitrogen fixation as a source of nitrogen to the North Atlantic Ocean. *Biogeochemistry* **35**: 261–274.

McGillicuddy DJ, Johnson R, Siegel DA, Michaels AF, Bates NR, Knap AH. (1999). Mesoscale variations of biogeochemical properties in the Sargasso Sea. *J Geophys Res Oceans* **104**: 13381–13394.

McGillicuddy DJ, Robinson AR. (1997). Eddy-induced nutrient supply and new production in the Sargasso Sea. *Deep Sea Res I* **44**: 1427–1450.

McGillicuddy DJ, Robinson AR, Siegel DA, Jannasch HW, Johnson R, Dickeys T *et al.* (1998). Influence of mesoscale eddies on new production in the Sargasso Sea. *Nature* **394**: 263–266.

McNeil JD, Jannasch HW, Dickey T, McGillicuddy D, Brzezinski M, Sakamoto CM. (1999). New chemical, bio-optical and physical observations of upper ocean response to the passage of a mesoscale eddy off Bermuda. *J Geophys Res Oceans* **104**: 15537–15548.

Michaels AF, Olson D, Sarmiento JL, Ammerman JW, Fanning K, Jahnke R *et al.* (1996). Inputs, losses and transformations of nitrogen and phosphorus in the pelagic North Atlantic Ocean. *Biogeochemistry* **35**: 181–226.

Montoya JP, Voss M, Kahler P, Capone DG. (1996). A simple, high-precision, high-sensitivity tracer assay for N_2 fixation. *Appl Environ Microbiol* **62**: 986–993.

Ohki K, Zehr JP, Fujita Y. (1992). Regulation of nitrogenase activity in relation to the light-dark regime in the filamentous nonheterocystous cyanobacterium *Trichodesmium* sp. NIBB 1067. *J Gen Microbiol* **138**: 2679–2685.

Postgate JR. (1982). *The Fundamentals of N_2 Fixation*. Cambridge University Press: Cambridge.

Sakamoto CM, Karl DM, Jannasch HW, Bidigare RR, Letelier RM, Walz PM *et al.* (2004). Influence of Rossby waves on nutrient dynamics and the plankton community structure in the North Pacific subtropical gyre. *J Geophys Res Oceans* **109**: C05032, doi:10.1029/2003JC001976.

Strickland JD, Parsons TR. (1972). *A Practical Handbook of Seawater Analysis*. Fisheries Research Board of Canada: Ottawa.

Sweeney EN, McGillicuddy DJ, Buesseler KO. (2003). Biogeochemical impacts due to mesoscale eddy activity in the Sargasso Sea as measured at the

Bermuda Atlantic Time-series Study (BATS). *Deep Sea Res II* **50**: 3017–3039.

Uz BM, Yoder JA, Osychny V. (2001). Pumping of nutrients to ocean surface waters by the action of propagating planetary waves. *Nature* **409**: 597–600.

Venrick EL. (1993). Phytoplankton seasonality in the central North Pacific—the endless summer reconsidered. *Limnol Oceanogr* **38**: 1135–1149.

Wyman M, Zehr JP, Capone DG. (1996). Temporal variability in nitrogenase gene expression in natural populations of the marine cyanobacterium *Trichodesmium thiebautii*. *Appl Environ Microbiol* **62**: 1073–1075.

Yentsch CS, Phinney DA. (1985). Rotary motions and convection as a means of regulating primary production in warm core rings. *J Geophys Res Oceans* **90**: 3237–3248.

Zehr JP, Mellon MT, Zani S. (1998). New nitrogen-fixing microorganisms detected in oligotrophic oceans by amplification of nitrogenase (*nifH*) genes. *Appl Environ Microbiol* **64**: 3444–3450.

Zehr JP, Turner PJ. (2001). Nitrogen fixation: Nitrogenase genes and gene expression. In: Paul JH (ed). *Methods in Microbiology*, Vol 30, Academic Press: San Diego, CA, USA, pp 271–286.

Zehr JP, Waterbury JB, Turner PJ, Montoya JP, Omoregie E, Steward GF *et al*. (2001). Unicellular cyanobacteria fix N_2 in the subtropical North Pacific Ocean. *Nature* **412**: 635–638.

Zehr JP, Wyman M, Miller V, Duguay L, Capone DG. (1993). Modification of the Fe Protein of nitrogenase in natural populations of *Trichodesmium thiebautii*. *Appl Environ Microbiol* **59**: 669–676.